DOI: 10.1002/chem.201000391

Promoted H_2 Generation from NH_3BH_3 Thermal Dehydrogenation Catalyzed by Metal–Organic Framework Based Catalysts

Yaoqi Li, Ping Song, Jie Zheng, and Xingguo Li*[a]

Abstract: The application of ammonium borane (AB) as a hydrogen storage material is limited by the sluggish kinetics of H_2 release. Two catalysts based on metal–organic frameworks (MOFs) have been prepared either by applying MOF as precursors or by the in situ reduction method. In the release of H_2 from AB, the high H_2 content of the whole system, the remarkably lower reaction onset temperature, the significantly increased H_2 release rates at $\leq 90\,^{\circ}C$, and the decreased reaction exothermicity have all been achieved with only 1.0 mol% MOF-based catalyst. Moreover, the clear catalytic diversity of three catalysts has been observed and discussed. The in situ synthesized Ni^0 sites and the MOF supports in the catalysts were proven to show significant and different effects to promote the catalytic activities. With MOF-based catalysts, both the enhanced kinetics and the high H_2 capacity of the AB system present great advantages for future use.

Keywords: heterogeneous catalysis · hydrogen · materials science · metal–organic frameworks

Introduction

On-board storage is a major technical barrier to the application of H_2 as a transportation fuel.[1] In recent years, ammonia borane (AB) has attracted increasing attention as an efficient and safe storage medium for H_2,[2–6] owing to the high capacity (19.6 wt% by weight and 0.145 kg L^{-1} by volume) and the stability in ambient atmosphere.[2,5] The practical application of AB as an on-board hydrogen medium is, however, limited by the sluggish dehydrogenation kinetics at $\leq 100\,^{\circ}C$,[7–9] Other drawbacks of AB include the release of by-products and the lack of cost-effective methods for spent fuel regeneration.[10] Recently, various remarkable approaches have been developed to promote the H_2 generation from AB, such as, catalytic hydrolysis in aqueous solution[11,12] and methanol,[l,13] dehydrocoupling in ionic liquids[14–16] or organic solvents,[6,17–19] tailoring nanophase structures by using nanoporous scaffolds,[20–22] substituting an H of NH_3 in AB by alkali or alkaline earth metals,[23–26] and catalytic thermal decomposition.[7,9,27] The solvents, ionic liquids, porous scaffolds, or the replacing metals inevitably bring additional weight to the whole system and thus decrease the overall hydrogen storage capacity. Therefore, the thermal decomposition of AB with a small amount of catalyst has become particularly attractive.[11,28] At present, one pending issue in the catalyzed thermal decomposition of AB is the kinetic rates at low temperatures (the most favorable is around 85 °C for proton exchange membrane fuel cell (PEMFC)). Efficient catalysts are thus essential for further development of the thermal dehydrogenation of AB.

Metal–organic frameworks (MOFs), structures composed of metal sites and organic ligands, have also been greatly focused on. The extremely large surface areas, abundant microporous pores, and uniform channels of MOFs have offered convenient conditions for small molecules to access the interior surface and react with each metal site independently. Therefore, MOFs by nature should promote the formation of active metal sites as well as provide a porous support for catalysis.

In our efforts to promote the thermal decomposition of AB, we have developed two MOF-based catalysts (MOFcats). A mild reduction method was introduced to synthesize the MOFcats from [Ni(4,4′-bipy)][HBTC] (4,4′-bipy = 4,4′-bipyridine, H_3BTC = 1,3,5-benzenetricarboxylic acid) (MOF1) and [Ni(pyz)][$Ni(CN)_4$] (pyz = pyrazine) (MOF2).

[a] Dr. Y. Li, Dr. P. Song, Prof. J. Zheng, Prof. X. Li
Beijing National Laboratory for Molecular Sciences (BNLMS)
(The State Key Laboratory of Rare Earth Materials Chemistry and Applications)
College of Chemistry and Molecular Engineering
Peking University, Beijing, 100871 (P.R. China)
Fax: (+86) 10-62765930
E-mail: xgli@pku.edu.cn

Supporting information for this article is available on the WWW under http://dx.doi.org/10.1002/chem.201000391.

The catalytic results reveal that both the in situ synthesis and the confinement of the active sites within microporous framework result in unexpected catalytic activities of the MOFcats.

Results and Discussion

The MOF-based catalysts (MOF1cat, MOF2cat, and MOF3cat) were synthesized by immersing the corresponding MOF (Figure 1) in a solution of AB in methanol. As illustrated in Figures S1–S9 in the Supporting Information, MOF1, MOF2, and MOF3 have been characterized by powder X-ray diffraction (XRD), thermal gravimetric analysis (TGA), and nitrogen sorption measurements, which show favorable crystallinity, high thermal stability, and ordered porous structures with large surface areas (1570, 1518, and 718 $m^2 g^{-1}$, respectively). The microporous frameworks of the MOFs promote the high dispersion of reactant molecules and offer channels for these molecules to infiltrate into the interior pores. In addition, the MOFs provide abundant metal and organic sites to absorb the reactant molecules. The special structures of the precursors (MOFs) promote the synthesis of the MOF-based catalysts.

AB has been shown to be an efficient and mild reducing reagent.[12,28,30] As shown in Figures S10 and S11 in the Supporting Information, when treated with a solution of AB in methanol, the green crystals of MOF1 and the purple powder of MOF2 gradually turn into black powders. Importantly, the Ni 2p X-ray photoelectron spectroscopy (XPS) peaks of the as-synthesized MOF1cat and MOF2cat, as shown in Figure 2, can be deconvoluted into two peaks at 852 and 856 eV, indicating the presence of both metallic Ni (852 eV) and divalent Ni (856 eV). The results reveal that in MOF1cat and MOF2cat, some of Ni^{2+} ions in the original MOFs have been reduced to zero valence Ni (852 eV) and

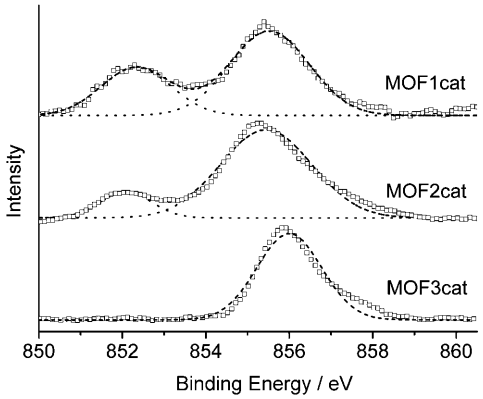

Figure 2. Ni 2p X-ray photoelectron spectra of MOF1cat, MOF2cat, and MOF3cat.

the Ni^{2+} peaks (856 eV) are ascribed to the remaining frameworks. The relative peak areas of Ni^0 (852 eV) and Ni^{2+} (856 eV) in XPS spectra indicate that more Ni^{2+} has been reduced to Ni^0 in MOF1cat than in MOF2cat, which is attributed to the relatively weak coordination between Ni^{2+} and the ligands in MOF1. Moreover, as shown in Figures S12 and S13 in the Supporting Information, the as-prepared MOF1cat and MOF2cat display the XPS peaks that are assigned to elemental C, N, O, and Ni. The C, N, and O elements, which belong to the organic ligands constructing the framework, further confirm the existence of some portion of the preserved MOF structures. As a result, owing to the microporous precursors (MOFs) and the mild reduction method, MOF1cat and MOF2cat contain both in situ synthesized Ni^0 sites and some preserved framework supports.

The structures of MOF1cat and MOF2cat were further studied by TEM and XRD. The TEM images of MOF1cat and MOF2cat are composed of nanosized particles (Figure 3). The rough and porous surfaces of the MOFcats

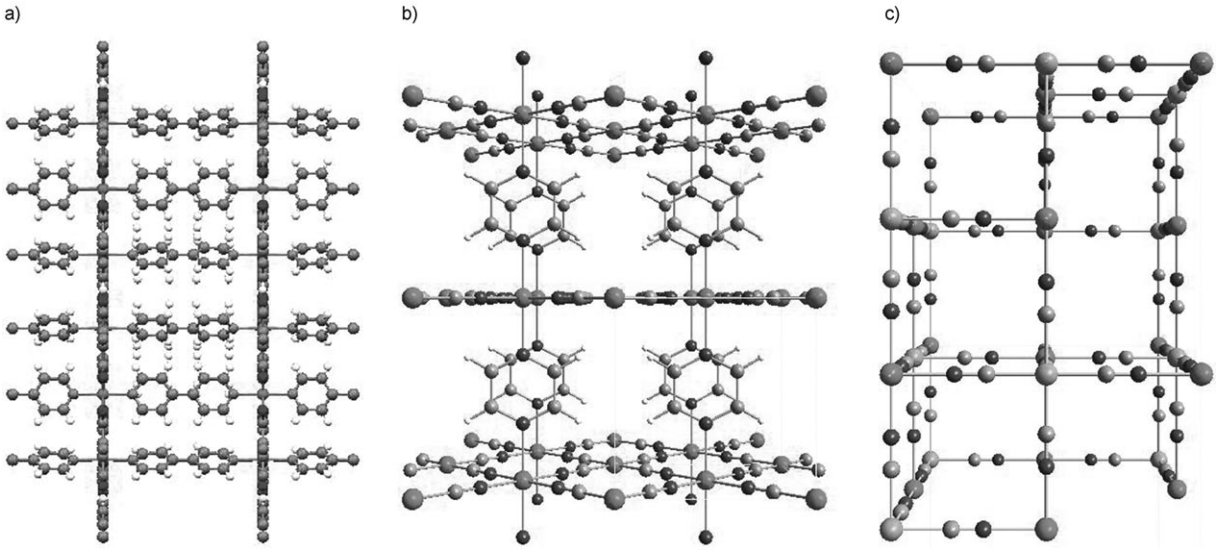

Figure 1. The frameworks of a) MOF1, b) MOF2, and c) MOF3.

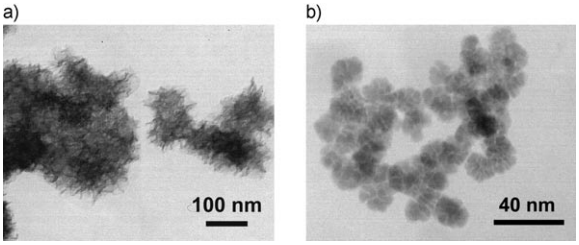

Figure 3. TEM images of the as-prepared a) MOF1cat and b) MOF2cat.

are caused by the in situ reduction reaction happening in the tiny pores and channels of the frameworks. The XRD patterns (Figure S1 in the Supporting Information) demonstrate that in MOF1cat, the as-prepared Ni^0 is in the amorphous phase and the remaining framework support exhibits poor crystallinity. Compared with that of MOF1cat, the microporous crystal structure of MOF2cat has been unexpectedly well kept during the synthetic process (Figure S2 in the Supporting Information). The MOF2cat consists of amorphous metallic Ni supported on the well-preserved microporous framework. The clear difference between the framework crystallinity of MOF1cat and that of MOF2cat is attributed to the reduction of more Ni^{2+} sites to Ni^0 in MOF1cat, as discussed previously. Meanwhile, the differential scanning calorimetry (DSC) curves of the as-synthesized MOFcats (Figure S14 in the Supporting Information) show no observable peaks from room temperature to 140 °C, which reveal that the catalysts have good thermal stability and the frameworks in the MOFcats can preserve their structures below 140 °C.

MOF3cat, although synthesized from a similar method, exhibits quite different properties to those of MOF1cat and MOF2cat. No significant color change of MOF 3 has been observed during the preparation (Figure S15 in the Supporting Information). In addition, the Ni 2p XPS spectrum of the as-prepared sample shows only one Ni^{2+} peak at 856 eV (Figure 2). It is ascribed to the strong bonds between metal ions and the CN ligands, which prevents the reduction reaction of Ni^{2+} in MOF3. The XRD patterns of MOF3cat further prove that there is no significant change of MOF3 after the synthetic process (Figure S3 in the Supporting Information).

In MOF1cat and MOF2cat, both the amorphous Ni^0 sites and the remaining frameworks could be anticipated to enhance the catalytic activities and promote the release of H_2 from AB, whereas the differences in the amount of Ni^0 sites and the framework supports of MOF1cat, MOF2cat, and MOF3cat should lead to varying catalytic behaviors, as shown below.

Each of the MOFcats was mixed with AB by hand in an agate mortar in a 1:100 molar ratio so as not to sacrifice the high overall gravimetric storage capacity. As shown in the DSC curves (Figure 4), neat AB released the first equivalent of H_2 at approximately 114 °C following the endothermic melting peak at approximately 109 °C, and the second equivalent of H_2 with a broad DSC peak centered a approximate-

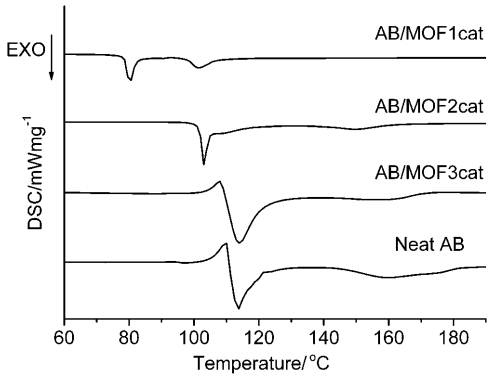

Figure 4. The DSC results of AB/MOF1cat, AB/MOF2cat, AB/MOF3cat, and neat AB.

ly 161 °C at a heating rate of 5 °C min^{-1}, in agreement with literature results.[3,5] In contrast, AB/MOF1cat (Figure 4) releases H_2 with one peak centered at 80 °C and another peak at 101 °C. For AB/MOF2cat, the decomposition occurs with a desorption DSC peak at 102 °C and gives a peak of very low intensity at around 150 °C. The disappearance of the endothermic melting peak indicates the direct solid-state dehydrogenation of AB/MOFcats. Importantly, MOF1cat lowers the dehydrogenation onset temperatures more effectively than MOF2cat; this is attributed to the existence of abundant amorphous Ni^0 in MOF1cat. As described previously, compared with MOF2cat, MOF1cat contains more metallic Ni^0 sites. During the synthesis of MOFcats, AB molecules gradually infiltrate into the microporous framework of the MOFs and reduce Ni^{2+} to the metallic form. The special structure of the MOFs containing Ni^{2+} sites, which are uniformly separated by organic ligands, allows for the reactant molecules to access and react with each Ni^{2+} ion in the frameworks separately. Therefore, the metallic Ni, generated from independent Ni^{2+} sites within the framework, is quite different from normal Ni nanomaterials and is likely present as very tiny clusters, which possess high catalytic activity. Additionally, the amorphous phase has a great structural distortion and aids in obtaining a high concentration of active sites for catalysis.[31,32] This effect of Ni^0 has been further proved by the results of MOF3cat. As mentioned previously, no Ni^0 in MOF3cat has been observed. Compared with those of AB/MOF1cat and AB/MOF2cat, the DSC curve of AB/MOF3cat shows no significant differences to that of neat AB. The results reveal that only with in situ synthesized Ni^0 sites, can the MOFcats greatly enhance the kinetics and efficiently lower the dehydrogenation temperatures.

For AB/MOF1cat and AB/MOF2cat, the second steps of desorption exhibit different DSC patterns (AB/MOF1cat with a relatively sharp peak and AB/MOF2cat with a peak of very low intensity) compared with that of neat AB. The difference in the mechanism of the first step in the thermal decomposition process should affect the behavior of the H_2 release in the second step. Furthermore, the DSC results of AB and AB/MOFcats illustrate that the decomposition re-

action enthalpies from AB/MOF1cat and AB/MOF2cat ($\Delta H = -4.3$ and -7.9 kJ mol^{-1}, respectively) are significantly less than that of neat AB ($\Delta H = -21$ kJ mol^{-1}).[8,20] The decreased reaction exothermicity favors the regeneration of the spent fuel. More importantly, the differences in the ΔH values, combined with the changes of DSC patterns indicate that the MOFcats with Ni^0 sites lead to a change in the thermodynamics of the thermal decomposition, which is probably the reason that the AB/MOFcats can generate H_2 at lower temperatures.

Isothermal volumetric H_2 release measurements also present distinct features among the neat and the MOFcat-doped AB samples. As shown in Figure 5a, little H_2 generation has been detected from neat AB after being held at 80 °C for 2.5 h, which is due to the long induction period for the formation of the initiator (the diammoniate of diborane)[9,33] and the high kinetic barrier of dehydrogenation. In contrast, AB/MOF1cat can release approximately 7.5 wt % H_2 within 2 h and AB/MOF2cat generates approximately 6.0 wt % H_2 within only 40 min at 80 °C. Importantly, the AB/MOF1cat does not suffer from the long induction period that is present in neat AB. Compared with AB/MOF1cat, after a short induction period of approximately 20 min, AB/MOF2cat evolves H_2 vigorously at a high release rate of 0.48 wt % per minute. One reason for the remarkably accelerated kinetics is the active Ni^0 sites. As mentioned above, in MOF1cat there exists abundant active metallic Ni^0 sites, which are proposed to be the catalytically active species. The sufficient amorphous Ni^0 sites in MOF1cat result in the fast H_2 evolution without any induction period. The different behavior in the dehydrogenation of the AB/MOF2cat is attributed to the preserved framework, which is naturally a good substrate for highly dispersed tiny metal clusters. Owing to the confinement effect of the microporous framework, in AB/MOF2cat, although the Ni^0 sites are not sufficient enough to reach a very low reaction onset temperature and a kinetic process without an induction period, the supporting effect of the well preserved MOF2 combined with Ni^0 leads to a further significant acceleration of the kinetics (0.48 wt % H_2 per minute) in AB/MOF2cat after the inevitable short induction period.

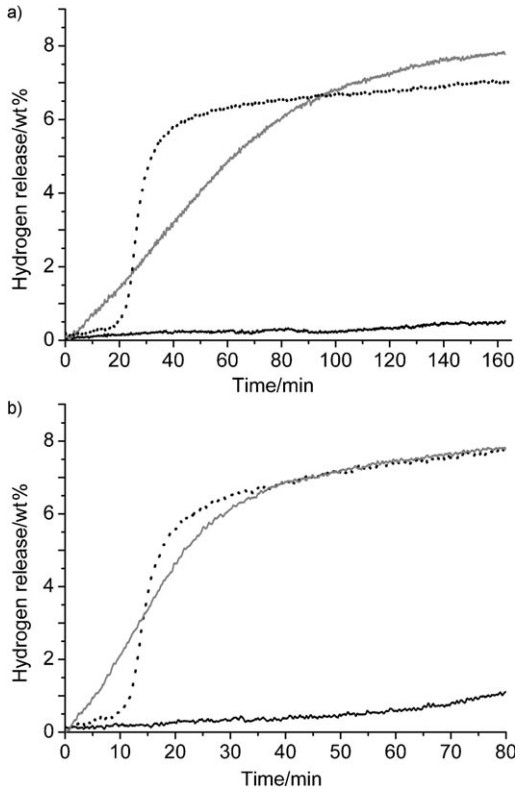

Figure 5. The volumetrically measured release of H_2 from AB/MOF1cat (gray line), AB/MOF2cat (dotted line), and neat AB (black line)at a) 80 °C and b) 90 °C.

At a higher temperature of 90 °C (Figure 5b), the AB/MOFcat samples present significantly fast kinetics. Approximately 7.0 wt % H_2 for AB/MOF1cat can be generated in 40 min without an induction period. For AB/MOF2cat, 6.0 wt % H_2 was vigorously released within only 20 min, whereas the corresponding release of H_2 from neat AB is less than 0.3 wt %. At the same operating temperatures, the dehydrogenation rate of AB/MOFcat is similar to that recently reported by Lu et al.[22] in the AB/Li^+–carbon composite (50:50 of AB and carbon), but the MOFcats (1.0 mol %) bring significantly less additional weight. Both the H_2 capacity and the H_2 release rate by weight of the whole system are much higher in the AB/MOFcats.

To obtain further insight into the enhanced kinetics, the activation energy has been determined by the Kissinger equation, namely,

$$\ln(\beta/T_p^2 = \ln(AR/E_a) - E_a/RT_p$$

in which β is the heating rate, T_p is the temperature of the maximum reaction rate peak, A is the pre-exponential factor, R is the gas constant, and E_a is the activation energy. As shown in Figure 6a and b, DSC tests have been performed with various heating rates and the dependences of $\ln(\beta/T_p^2)$ versus $1000/T_p$ are shown to in Figure 6c. The activation energies for the H_2 release of AB/MOF1cat and AB/MOF2cat are determined to be approximately (131 ± 5) and (160 ± 5) kJ mol^{-1}, respectively, which are lower than that of the neat AB ((184 ± 5) kJ mol^{-1}).[20] The decrease in the E_a value of the AB/MOFcats further provides direct evidence for the possibility of enhancing the kinetics of the AB decomposition with MOFcats.

The development of good catalysts is an essential step towards the application of the AB-based hydrogen storage system. The above results suggest that MOF1cat and MOF2cat provide an effective strategy to modify the enthalpy of decomposition and speed up the kinetics in the thermal dehydrogenation of AB. The in situ generation of metal clusters in the catalysts prepared from different MOFs provides a novel strategy to produce catalytically active metal sites. The microporous structures of the MOFs have been found to be good substrates for highly dispersed tiny metal

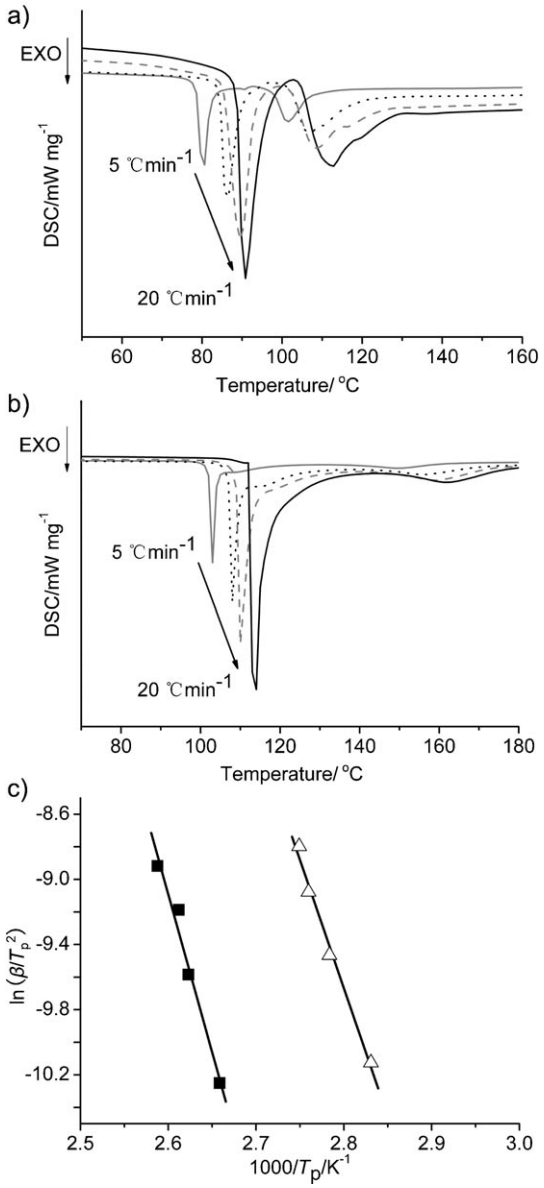

Figure 6. DSC profiles of the dehydrogenation of a) AB/MOF1cat and b) AB/MOF2cat at heating rates of 5, 10, 15, and 20 °C min^{-1}. c) The Kissinger plots of the MOF1cat-doped (△) and MOF2cat-doped (■) AB samples.

clusters. Due to the good thermal stability of the frameworks and the MOFcats (Figures S4, S5, S6, and S14 in the Supporting Information) during the thermal dehydrogenation of the AB/MOFcats at 80 and 90 °C, the remaining frameworks in the MOFcats should not be destroyed by the heating process. Moreover, because AB itself is a mild reducing reagent, it is possible that some Ni^{2+} in the MOFcats could be further reduced to Ni^0 sites, which are catalytically active and thus promote the activity of the MOFcats. MOF1cat with abundant amorphous Ni^0 sites leads to the rapid release of H_2 from AB without any induction period. MOF2cat with a well-preserved framework can further remarkably accelerate the H_2 release rate. MOF3cat without Ni^0 sites shows no significant catalytic activity in the decomposition. The clearly distinct catalytic activities of the three catalysts, caused by different catalytic effects of Ni^0 sites and the preserved framework, are attributed to the different structures and organic ligands of original MOFs. If the coordination between the ligands and the metal ions in the MOFs is weak, as in MOF1cat, Ni^{2+} can be easily reduced to amorphous Ni^0 along with some destruction of the framework. For the MOFs constructed by very strongly bound ligands, it is, however, difficult to obtain catalytically active metallic sites (Ni^0), as shown in MOF3cat. For future development, by adopting proper metal ions, organic ligands, and reducing agents, we may find a suitable MOF for which the corresponding MOFcat contains both sufficient active Ni^0 sites and a properly preserved MOF support. This new MOFcat should in principle further enhance the catalytic activity and kinetics in the dehydrogenation of AB. Further investigations on more MOFcats are needed.

Conclusion

Two novel MOFcats synthesized from microporous MOFs, have been introduced into an AB thermal dehydrogenation system. The in situ synthesized Ni^0 sites and the preserved framework supports in the MOFcats greatly promote the catalytic activity.

Catalyzed by MOFcats (1.0 mol %), the decomposition of AB shows a significantly lower reaction onset temperature, decreased activation energy, and remarkably accelerated kinetics. At 80 °C, AB with MOF1-based catalyst (MOF1cat) released 7.5 wt % H_2 in 2 h without any induction period. Catalyzed by MOF2-based catalyst (MOF2cat) at 80 °C, AB can generate 6.0 wt % H_2 in 40 min. At 90 °C, approximately 7.0 wt % H_2 for MOF1cat doped AB (AB/MOF1cat) within 40 min and 6.0 wt % H_2 for MOF2cat doped AB (AB/MOF2cat) within only 20 min can be vigorously released. Moreover, the results indicate that the compositional and structural diversity of three MOFs (MOF1, MOF2, and $Ni_3[Fe(CN)_6]_2$ (MOF3)) leads to clearly distinct catalytic activities and behaviors of the corresponding MOFcats. Therefore, for further development, both the frameworks and the metal sites in the MOFs can be well adjusted by crystal engineering[29] to create more effective MOFcats for various catalytic processes.

The catalytic effects of the MOFcats make AB a competitive candidate for hydrogen storage and the study of three MOFcats implies a novel type of efficient catalysts. The significantly different catalytic activities of the MOFcats, which are attributed to the different effects of the Ni^0 sites and the preserved MOF support, present great potential for future development. Not only the catalytic efficiency of MOFcats, but also the huge componential and structural diversity of MOFs provide us enormous possibilities for a variety of catalyst designs.

Experimental Section

Synthesis of MOF1, MOF2, and MOF3: MOF1 and MOF2 were synthesized according to our previous work.[34,35] MOF3 was prepared by solution reaction at ambient temperature (see the Supporting Information). MOF 1, 2, and 3 were identified by powder XRD (Rigaku D/Max2500 VB2+PC). Thermogravimetric analyses (TGA) were carried out on a TGA-DSC-DTA (Q600 SDT) analyzer with a heating rate of 5 °C min^{-1} under an N_2 atmosphere. After the activation process (180 °C, 2 h for MOF1; 220 °C, 4 h for MOF2; and 200 °C 4 h for MOF3), N_2 sorptions measurements were taken on a COULTER SA 3100 apparatus at −196 °C.

Synthesis of MOF-based catalysts: MOF1cat, MOF2cat, and MOF3cat were synthesized by immersing the corresponding MOF into a solution of AB in methanol (the molar ratio of MOF/AB = 0.02) in a glove box at room temperature for a week. The products were filtered and washed with five 10 mL portions of methanol and dried under Ar. The as-synthesized catalysts were identified by XRD, X-ray photoelectron spectroscopy (XPS), and TEM. The XPS experiments were conducted on an AXIS-Ultra instrument from Kratos Analytical using monochromatic $Al_{K\alpha}$ radiation (225 W, 15 mA, 15 kV) and low-energy electron flooding for charge compensation. The TEM micrographs were performed on a JEM-200CX machine.

Catalytic measurements of MOF-based catalysts: The MOFcats were mixed with AB by hand in an agate mortar for 3 min in a glove box at room temperature. The molar ratio of the MOFcat/AB = 0.010. DSC was carried out under a flowing stream of Ar at a Netzsch DSC 204 HP calorimeter. The H_2 generated from the thermal decomposition of the MOFcat-doped AB was measured by a pressure capacity temperature (PCT) measuring system, based on the volumetric method.

Acknowledgements

The authors acknowledge NSFC (Nos. 20971009 and 20821091) and MOST of China (No. 2009CB939902 and 2010CB631301).

[1] L. Schlapbach, A. Zuttel, *Nature* **2001**, *414*, 353–358.
.
[2] T. B. Marder, *Angew. Chem.* **2007**, *119*, 8262–8264; *Angew. Chem. Int. Ed.* **2007**, *46*, 8116–8118.
[3] F. H. Stephens, V. Pons, R. T. Baker, *Dalton Trans.* **2007**, 2613–2626.
[4] B. Peng, J. Chen, *Energy Environ. Sci.* **2008**, *1*, 479–483.
[5] C. W. Hamilton, R. T. Baker, A. Staubitz, I. Manners, *Chem. Soc. Rev.* **2009**, *38*, 279–293.
[6] F. H. Stephens, R. T. Baker, M. H. Matus, D. J. Grant, D. A. Dixon, *Angew. Chem.* **2007**, *119*, 760–763; *Angew. Chem. Int. Ed.* **2007**, *46*, 746–749.
[7] M. G. Hu, R. A. Geanangel, W. W. Wendlandt, *Thermochim. Acta* **1978**, *23*, 249–255.
[8] G. Wolf, J. Baumann, F. Baitalow, F. P. Hoffmann, *Thermochim. Acta* **2000**, *343*, 19–25.
[9] M. Bowden, T. Autrey, I. Brown, M. Ryan, *Curr. Appl. Phys.* **2008**, *8*, 498–500.
[10] B. L. Davis, D. A. Dixon, E. B. Garner, J. C. Gordon, M. H. Matus, B. Scott, F. H. Stephens, *Angew. Chem.* **2009**, *121*, 6944–6948; *Angew. Chem. Int. Ed.* **2009**, *48*, 6812–6816.
[11] F. Y. Cheng, H. Ma, Y. M. Li, J. Chen, *Inorg. Chem.* **2007**, *46*, 788–794.
[12] J. M. Yan, X. B. Zhang, S. Han, H. Shioyama, Q. Xu, *Angew. Chem.* **2008**, *120*, 2319–2321; *Angew. Chem. Int. Ed.* **2008**, *47*, 2287–2289.
[13] S. B. Kalidindi, U. Sanyal, B. R. Jagirdar, *Phys. Chem. Chem. Phys.* **2008**, *10*, 5870–5874.
[14] M. E. Bluhm, M. G. Bradley, R. Butterick, U. Kusari, L. G. Sneddon, *J. Am. Chem. Soc.* **2006**, *128*, 7748–7749.
[15] D. W. Himmelberger, L. R. Alden, M. E. Bluhm, L. G. Sneddon, *Inorg. Chem.* **2009**, *48*, 9883–9889.
[16] D. W. Himmelberger, C. W. Yoon, M. E. Bluhm, P. J. Carroll, L. G. Sneddon, *J. Am. Chem. Soc.* **2009**, *131*, 14101–14110.
[17] M. C. Denney, V. Pons, T. J. Hebden, D. M. Heinekey, K. I. Goldberg, *J. Am. Chem. Soc.* **2006**, *128*, 12048–12049.
[18] R. J. Keaton, J. M. Blacquiere, R. T. Baker, *J. Am. Chem. Soc.* **2007**, *129*, 1844–1845.
[19] M. Käß, A. Friedrich, M. Drees, S. Schneider, *Angew. Chem.* **2009**, *121*, 922–924; *Angew. Chem. Int. Ed.* **2009**, *48*, 905–907.
[20] A. Gutowska, L. Y. Li, Y. S. Shin, C. M. M. Wang, X. H. S. Li, J. C. Linehan, R. S. Smith, B. D. Kay, B. Schmid, W. Shaw, M. Gutowski, T. Autrey, *Angew. Chem.* **2005**, *117*, 3644–3648; *Angew. Chem. Int. Ed.* **2005**, *44*, 3578–3582.
[21] A. Feaver, S. Sepehri, P. Shamberger, A. Stowe, T. Autrey, G. Z. Cao, *J. Phys. Chem. B* **2007**, *111*, 7469–7472.
[22] L. Li, X. Yao, C. H. Sun, A. J. Du, L. N. Cheng, Z. H. Zhu, C. Z. Yu, J. Zou, S. C. Smith, P. Wang, H. M. Cheng, R. L. Frost, G. Q. M. Lu, *Adv. Funct. Mater.* **2009**, *19*, 265–271.
[23] Z. T. Xiong, C. K. Yong, G. T. Wu, P. Chen, W. Shaw, A. Karkamkar, T. Autrey, M. O. Jones, S. R. Johnson, P. P. Edwards, W. I. F. David, *Nat. Mater.* **2008**, *7*, 138–141.
[24] H. V. K. Diyabalanage, R. P. Shrestha, T. A. Semelsberger, B. L. Scott, M. E. Bowden, B. L. Davis, A. K. Burrell, *Angew. Chem.* **2007**, *119*, 9153–9155; *Angew. Chem. Int. Ed.* **2007**, *46*, 8995–8997.
[25] J. Spielmann, G. Jansen, H. Bandmann, S. Harder, *Angew. Chem.* **2008**, *120*, 6386–6391; *Angew. Chem. Int. Ed.* **2008**, *47*, 6290–6295.
[26] X. D. Kang, Z. Z. Fang, L. Y. Kong, H. M. Cheng, X. D. Yao, G. Q. Lu, P. Wang, *Adv. Mater.* **2008**, *20*, 2756–2759.
[27] V. Sit, R. A. Geanangel, W. W. Wendlandt, *Thermochim. Acta* **1987**, *113*, 379–382.
[28] T. He, Z. T. Xiong, G. T. Wu, H. L. Chu, C. Z. Wu, T. Zhang, P. Chen, *Chem. Mater.* **2009**, *21*, 2315–2318.
[29] D. Braga, L. Brammer, N. R. Champness, *CrystEngComm* **2005**, *7*, 1–19.
[30] Y. Q. Li, L. Xie, Y. Li, J. Zheng, X. G. Li, *Chem. Eur. J.* **2009**, *15*, 8951–8954.
[31] J. F. Deng, H. X. Li, W. J. Wang, *Catal. Today* **1999**, *51*, 113–125.
[32] H. Cao, S. L. Suib, *J. Am. Chem. Soc.* **1994**, *116*, 5334–5342.
[33] A. C. Stowe, W. J. Shaw, J. C. Linehan, B. Schmid, T. Autrey, *Phys. Chem. Chem. Phys.* **2007**, *9*, 1831–1836.
[34] Y. Q. Li, L. Xie, Y. Liu, R. Yang, X. G. Li, *Inorg. Chem.* **2008**, *47*, 10372–10377.
[35] Y. Li, Y. Liu, Y. T. Wang, Y. H. Leng, L. Xie, X. G. Li, *Int. J. Hydrogen Energy* **2007**, *32*, 3411–3415.

Received: February 12, 2010
Revised: April 26, 2010
Published online: July 21, 2010

